



Confirmation of Large Super-fast Rotator (144977) 2005 EC₁₂₇

Chan-Kao Chang¹, Hsing-Wen Lin¹, Wing-Huen Ip^{1,2}, Zhong-Yi Lin³, Thomas Kupfer³, Thomas A. Prince³,
Quan-Zhi Ye^{3,4}, Russ R. Laher⁴, Hee-Jae Lee^{5,6}, and Hong-Kyu Moon⁶

¹Institute of Astronomy, National Central University, Jhongli, Taiwan; rex@astro.ncu.edu.tw

²Space Science Institute, Macau University of Science and Technology, Macau

³Division of Physics, Mathematics and Astronomy, California Institute of Technology, Pasadena, CA 91125, USA

⁴Infrared Processing and Analysis Center, California Institute of Technology, Pasadena, CA 91125, USA

⁵Department of Astronomy and Space Science, Chungbuk National University, 1, Chungdae-ro, Seowon-Gu, Cheongju, Chungbuk 28644, Korea

⁶Korea Astronomy and Space Science Institute, 776, Daedeok-daero, Yuseong gu, Daejeon 305-348, Korea

Received 2017 April 2; revised 2017 April 24; accepted 2017 April 27; published 2017 May 10

Abstract

(144977) 2005 EC₁₂₇ is a V-/A-type inner-main-belt asteroid with a diameter of 0.6 ± 0.1 km. Asteroids of this size are believed to have rubble-pile structure, and therefore cannot have a rotation period shorter than 2.2 hr. However, our measurements show that asteroid 2005 EC₁₂₇ completes one rotation in 1.65 ± 0.01 hr with a peak-to-peak light-curve variation of ~ 0.5 mag. Therefore, this asteroid is identified as a large super-fast rotator. Either a rubble-pile asteroid with a bulk density of $\rho \sim 6$ g cm⁻³ or an asteroid with an internal cohesion of 47 ± 30 Pa can explain 2005 EC₁₂₇. However, the scenario of high bulk density is very unlikely for asteroids. To date, only six large super-fast rotators, including 2005 EC₁₂₇, have been reported, and this number is very small when compared with the much more numerous fast rotators. We also note that none of the six reporting large SFRs are classified as C-type asteroids.

Key words: minor planets, asteroids: individual (144977) 2005 EC₁₂₇

1. Introduction

The large (i.e., a diameter of a few hundreds of meters) super-fast rotators (SFRs) are of interest for understanding asteroid interior structure. Because asteroids of sub-kilometer size are believed to have rubble-pile structure (i.e., gravitationally bounded aggregations) and cannot have super-fast rotation, defined as a rotation period shorter than 2.2 hr (Harris 1996).⁷ However, the first large SFR, 2001 OE84, a near-Earth asteroid of ~ 0.7 km in size and completing one rotation in 29.19 minutes (Pravec et al. 2002), cannot be explained by rubble-pile structure, and consequently, internal cohesion was proposed to be a possible solution (Holsapple 2007). Although several attempts were made to discover large SFRs with extensive-sky surveys (Masiero et al. 2009; Dermawan et al. 2011), this asteroid group was not confirmed until another large SFR, 2005 UW163, was found by Chang et al. (2014b). Up to now, five large SFRs have been reported, additionally including 1950 DA (Rozitis et al. 2014), 2000 GD65 (Polishook et al. 2016), and 1999 RE88 (Chang et al. 2016). However, the population size of large SFRs is still not clear. Compared with the 738 large fast rotators (i.e., diameters between 0.5 and 10 km and rotation periods between 2–3 hr) in the up-to-date Asteroid Light Curve Database (LCDB⁸; Warner et al. 2009), large SFRs are rare. Either the difficulty of discovering them due to their sub-kilometer sizes (i.e., relatively faint) or the intrinsically small population size of this group could lead to this rarity in detection. Therefore, a more comprehensive survey of asteroid rotation period with a wider sky coverage and a deeper limiting magnitude, such as the ZTF,⁹ could help in finding more large SFRs. With more

SFR samples, a thorough study of their physical properties could be conducted, and therefore further insights about asteroid interior structure are possible. To this objective, the TANGO project¹⁰ has been conducting asteroid rotation-period surveys since 2013 using the iPTF¹¹ (for details, see Chang et al. 2014a, 2015, 2016). From these surveys, 2 large SFRs and 27 candidates were discovered. Here, we report the confirmation of asteroid (144977) 2005 EC₁₂₇ as a new large SFR. The super-fast rotation of (144977) 2005 EC₁₂₇ was initially and tentatively identified in the asteroid rotation-period survey using the iPTF in 2015 February (Chang et al. 2016), and then later confirmed in this work by follow-up observations using the Lulin One-meter Telescope in Taiwan (LOT; Kinoshita et al. 2005).

This Letter is organized as follows. The observations and measurements are given in Section 2, the rotation period analysis is described in Section 3, the results and discussion are presented in Section 4, and a summary and conclusions can be found in Section 5.

2. Observations

The iPTF, LOT, and spectroscopic observations that support the findings in this work are described in this section. The details of each of these observation runs are summarized in Table 1.

2.1. iPTF Observations

The iPTF is a follow-up project of the PTF, a project whose aim is to explore the transient and variable sky synoptically. The iPTF/PTF employ the Palomar 48 inch Oschin Schmidt Telescope and an 11-chip mosaic CCD camera with a field of view of ~ 7.26 deg² (Law et al. 2009; Rau et al. 2009). This

⁷ The 2.2 hr spin barrier was calculated for an asteroid with a bulk density of $\rho = 3$ g cm⁻³.

⁸ <http://www.minorplanet.info/lightcurvedatabase.html>

⁹ Zwicky Transient Facility; <http://ptf.caltech.edu/ztf>.

¹⁰ Taiwan New Generation OIR Astronomy.

¹¹ Intermediate Palomar Transient Factory; <http://ptf.caltech.edu/iptf>.

Table 1
Observational Details

Telescope	Date	Filter	R.A. (°)	Decl. (°)	N_{exp}	Δt (hr)	α (°)	r (au)	Δ (au)	m (mag)	H (mag)
PTF	2015 Feb 25–26	R'	154.04	10.12	43	28.3	1.3	2.45	1.46	20.3	17.3
LOT	2016 Sept 24	r'	23.81	2.81	84	7.3	2.5	2.03	1.03	19.2	17.3
P200	2016 Oct 4	Spec.: $0.4 - 0.9 \mu\text{m}$	23.65	2.21	3	0.5	7.7	2.05	1.07	19.5	

Note. Δt is observation time span and N_{exp} is the total number of exposures.

wide field of view is extremely useful in collecting a large number of asteroid light curves within a short period of time. Four filters are currently available, including a Mould- R , Gunn- g' , and two different $H\alpha$ bands. The exposure time of the PTF is fixed at 60 s, which routinely reaches a limiting magnitude of $R \sim 21$ mag at the 5σ level (Law et al. 2010). All iPTF exposures are processed by the IPAC-PTF photometric pipeline (Grillmair et al. 2010; Laher et al. 2014), and the Sloan Digital Sky Survey fields (York et al. 2000) are used in the magnitude calibration. Typically, an accuracy of ~ 0.02 mag can be reached for photometric nights (Ofek et al. 2012a, 2012b). Since the magnitude calibration is done on a per-night, per-filter, per-chip basis, small photometric zero-point variations are present in PTF catalogs for different nights, fields, filters, and chips.

In the asteroid rotation-period survey conducted on 2015 February 25–26, we repeatedly observed six consecutive PTF fields near the ecliptic plane, in the R -band with a cadence of ~ 10 minutes. Asteroid 2005 EC₁₂₇ was observed in the PTF field centered at R.A. = 154°04 and decl. = 10°12 when it was approaching its opposition at a low phase angle of $\alpha \sim 1.3$. After all stationary sources were removed from the source catalogs, the light curves for known asteroids were extracted using a radius of $2''$ to match with the ephemerides obtained from the *JPL/HORIZONS* system. The light curve of 2005 EC₁₂₇ contains 42 clean detections from this observation run (i.e., the detections flagged as defective by the IPAC-PTF photometric pipeline were not included in the light curve).

2.2. LOT Observations

The follow-up observations to confirm the rotation period of 2005 EC₁₂₇ were carried out on 2016 September 24, using the LOT when 2005 EC₁₂₇ had a magnitude of $r' \sim 19.2$ at its low phase angle of $\alpha \sim 2.6$. The average seeing during the observations was $\sim 1.3''$. All images were taken in the r' -band with a fixed exposure time of 300 s using the Apogee U42 camera, a $2K \times 2K$ charge-coupled device with a pixel scale of $0.35''$. We acquired a total of 84 exposures over a time span of ~ 440 minutes, and the time difference between consecutive exposures was ~ 5 minutes. The image processing and reduction included standard procedures of bias and flat-field corrections, astrometric calibration using *astrometry.net*,¹² and aperture photometry using SExtractor (Bertin & Arnouts 1996). The photometric calibration was done against Pan-STARRS1 point sources of $r' \sim 14$ –22 mag (Magnier et al. 2016) using linear least-squares fitting, which typically achieved a fitting residual of ~ 0.01 mag. We improved the photometric accuracy by employing the trail-fitting method (Vereš et al. 2012; Lin et al. 2015) to accommodate the streaked image of 2005 EC₁₂₇ as a result of asteroid motion over the 300 s exposure time.

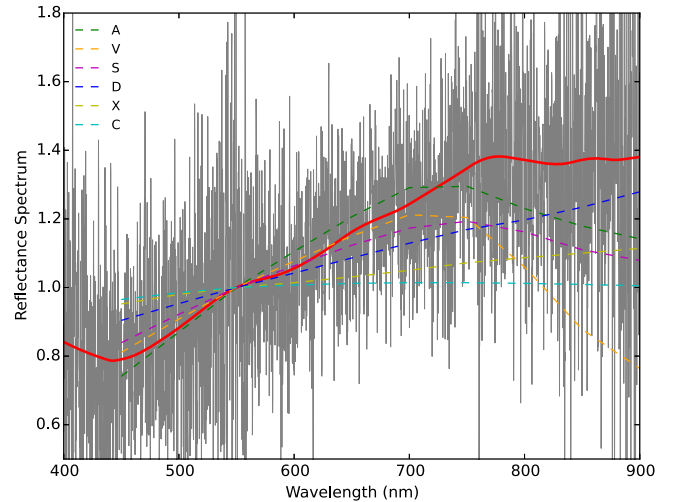


Figure 1. Reflectance spectrum of 2005 EC₁₂₇ taken by the P200. The gray line is the original reflectance spectrum and the red line is the running average using locally weighted scatter-plot smoothing (LOWESS; Cleveland 1979). The colored dashed lines are the reference spectra of A-type (green), V-type (orange), S-type (magenta), D-type (blue), X-type (yellow), and C-type (cyan) asteroids obtained from DeMeo et al. (2009). All spectra are normalized at wavelength 500 nm.

2.3. Spectroscopic Observations

To determine the taxonomic type for 2005 EC₁₂₇, its optical spectra were obtained using the Palomar 200 inch Hale Telescope (hereafter P200) and the Double-beam Spectrograph (Oke & Gunn 1982) in low-resolution mode ($R \sim 1500$). Three consecutive exposures were taken on 2016 October 4, with an exposure time of 300 s each. An average bias frame was made out of 10 individual bias frames and a normalized flat-field frame was constructed out of 10 individual lamp flat-field exposures. For the blue and red arms, respectively, FeAr and HeNeAr arc exposures were taken at the beginning of the night. Both arms of the spectrograph were reduced using a custom PyRAF-based pipeline¹³ (Bellm & Sesar 2016). The pipeline performs standard image processing and spectral reduction procedures, including bias subtraction, flat-field correction, wavelength calibration, optimal spectral extraction, and flux calibration. The average spectrum of 2005 EC₁₂₇ was constructed by combining all individual exposures, and then it was divided by the solar spectrum¹⁴ to obtain the reflectance spectrum of 2005 EC₁₂₇ (Figure 1). The trend of the reflectance spectrum suggests a V-/A-type asteroid for 2005 EC₁₂₇, according to the Bus-DeMeo classification scheme (DeMeo et al. 2009).

¹³ <https://github.com/ebellm/pyraf-dbsp>

¹⁴ The solar spectrum was obtained from Kurucz et al. (1984) and was then convolved with a Gaussian function to match the resolution of the spectrum of 2005 EC₁₂₇.

¹² <http://astrometry.net>

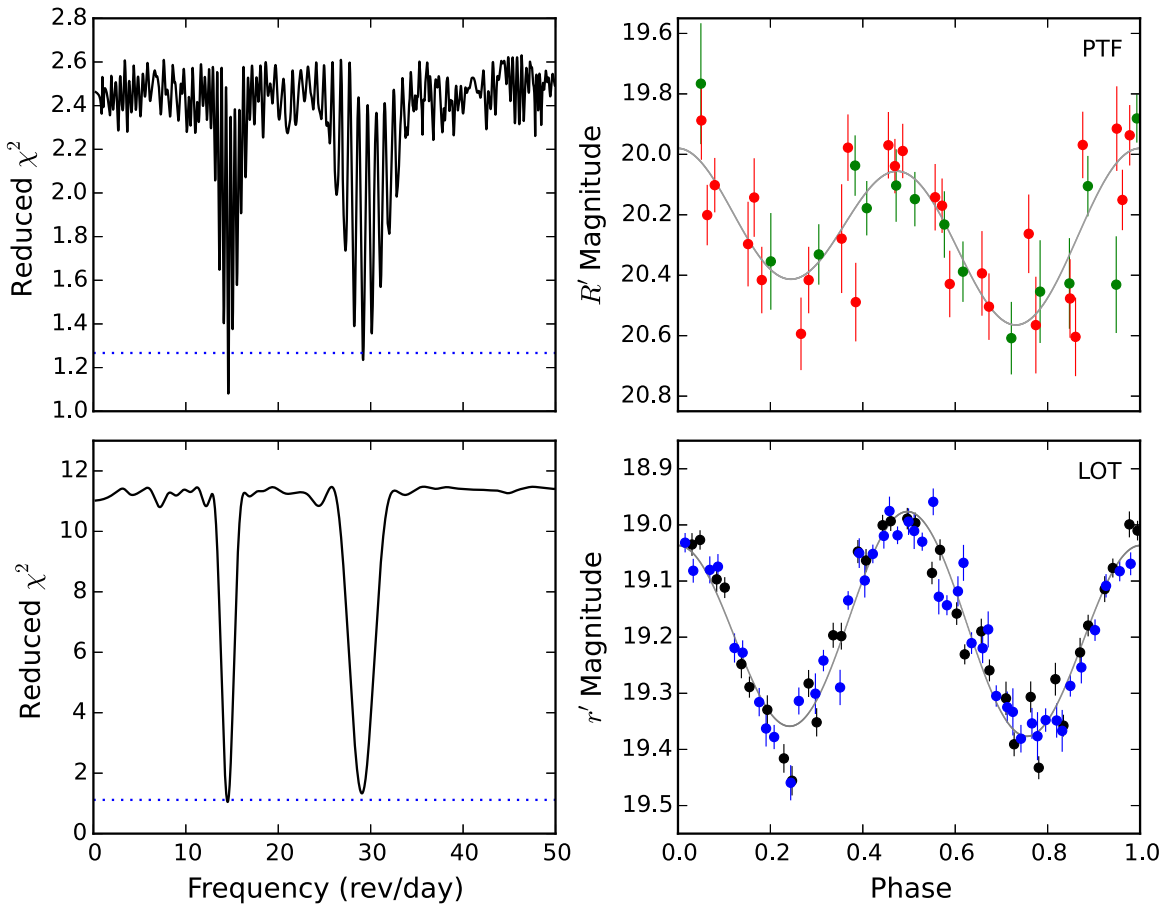


Figure 2. Periodograms (left) and folded light curves (right) for 2005 EC₁₂₇ obtained from iPTF (upper) and LOT (lower) observations. The blue dotted lines in the periodograms indicate the uncertainties in the derived rotation periods. The gray lines in the light curves are the fitted results. The green and red filled circles in the PTF light curve are data points obtained from 2015 February 25 and 26, respectively. The black and blue filled circles in the LOT light curve are data points of the even and odd rotation cycles, respectively.

3. Rotation-period Analysis

Before measuring the synodic rotation period for 2005 EC₁₂₇, the light-curve data points were corrected for light-travel time and were reduced to both heliocentric (r) and geocentric (Δ) distances at 1 au by $M = m + 5 \log(r\Delta)$, where M and m are reduced and apparent magnitudes, respectively. A second-order Fourier series (Harris et al. 1989) was then applied to search for the rotation periods:

$$M_{i,j} = \sum_{k=1,2}^{N_k} B_k \sin \left[\frac{2\pi k}{P} (t_j - t_0) \right] + C_k \cos \left[\frac{2\pi k}{P} (t_j - t_0) \right] + Z_i, \quad (1)$$

where $M_{i,j}$ is the reduced magnitude measured at the light-travel-time-corrected epoch, t_j ; B_k and C_k are the Fourier coefficients; P is the rotation period; t_0 is an arbitrary epoch; and Z_i is the zero point. For the PTF light curve, the fitting of Z_i also includes a correction for the small photometric zero-point variations mentioned in Section 2.1 (for details, see Polishook et al. 2012). To obtain the other free parameters for a given P , we used least-squares minimization to solve Equation (1). The frequency range was explored between 0.25 and 50 rev day⁻¹ with a step of 0.001 rev day⁻¹. To estimate the

uncertainty of the derived rotation periods, we calculated the range of periods with χ^2 smaller than $\chi_{\text{best}}^2 + \Delta\chi^2$, where χ_{best}^2 is the chi-squared value of the picked-out period and $\Delta\chi^2$ is obtained from the inverse chi-squared distribution, assuming $1 + 2N_k + N_i$ degrees of freedom.

The rotation period of 1.64 ± 0.01 hr (i.e., 14.6 rev day⁻¹) of 2005 EC₁₂₇ was first identified using the PTF light curve (Chang et al. 2016). Although the derived frequency of 14.6 rev day⁻¹ is significant in the periodogram calculated from the PTF light curve, the corresponding folded light curve is relatively scattered (see the upper panels of Figure 2). Therefore, we triggered the follow-up observations using the LOT. The rotation periods of 2005 EC₁₂₇ derived from the LOT light curve is 1.65 ± 0.01 hr (i.e., 14.52 rev day⁻¹), which is in good agreement with the PTF result (see the lower panels of Figure 1). Both folded light curves show a clear double-peak/valley feature for asteroid rotation (i.e., two periodic cycles). The peak-to-peak variations of the PTF and LOT light curves are ~ 0.6 and ~ 0.5 mag, respectively. This indicates that 2005 EC₁₂₇ is a moderately elongated asteroid and rules out the possibility of an octahedral shape for 2005 EC₁₂₇, which would lead to a light curve with four peaks and an amplitude of $\Delta m < 0.4$ mag (Harris et al. 2014). Moreover, we cannot morphologically distinguish between the even and odd cycles in the LOT light curve. Therefore, we believe that 1.65 hr is the true rotation period for 2005 EC₁₂₇.

4. Results and Discussion

To estimate the diameter, D , of 2005 EC₁₂₇, we use

$$D = \frac{1329}{\sqrt{p_v}} 10^{-H/5} \quad (2)$$

(see Harris & Lagerros 2002, and references therein). Since the phase angle of the asteroid had a small change during our relatively short observation time span, the absolute magnitude of 2005 EC₁₂₇ is simply calculated using a fixed G slope of 0.15 in the H - G system (Bowell et al. 1989). We obtain $H_{R'} = 17.27 \pm 0.22$ and $H_V = 17.30 \pm 0.02$ mag from the PTF and LOT observations, respectively.¹⁵ Because the absolute magnitude derived from the LOT observation has a smaller dispersion, we finally adopt $H_V = 17.30$ mag for 2005 EC₁₂₇. We use $(V - R) = 0.516$ in the conversion of $H_{R'}$ to H_V (DeMeo et al. 2009; Pravec et al. 2012) and then obtain $H_V = 17.82$ for 2005 EC₁₂₇. Assuming an albedo value of $p_v = 0.36 \pm 0.10$ for V-type and $p_v = 0.19 \pm 0.03$ for A-type asteroids (Masiero et al. 2011; DeMeo & Carry 2013), diameters of $D \sim 0.6 \pm 0.1$ and $\sim 0.8 \pm 0.1$ km, respectively, are estimated for 2005 EC₁₂₇, where the uncertainty includes the residuals in light-curve fitting and the range of assumed albedos. Even when an extreme albedo value of $p_v = 1.0$ is applied, a diameter of 0.4 km is still obtained for 2005 EC₁₂₇. Since A-type asteroids are relatively uncommon in the inner main belt, we therefore assume an V-type asteroid for 2005 EC₁₂₇ in the following discussion. As shown in Figure 4, 2005 EC₁₂₇ lies in the rubble-pile asteroid region and has a rotation period shorter than 2 hr. Therefore, we conclude that 2005 EC₁₂₇ is a large SFR.

If 2005 EC₁₂₇ is a rubble-pile asteroid, a bulk density of $\rho \sim 6 \text{ g cm}^{-3}$ would be required to withstand its super-fast rotation (see Figure 3). This would suggest that 2005 EC₁₂₇ is a very compact object, i.e., composed mostly of metal. However, such high bulk density is very unusual among asteroids. Moreover, 2005 EC₁₂₇ is probably a V-type asteroid. Therefore, this is a very unlikely scenario indeed.

Another possible explanation for the super-fast rotation of 2005 EC₁₂₇ is that it has substantial internal cohesion (Holsapple 2007; Sánchez & Scheeres 2014). Using the Drucker-Prager yield criterion,¹⁶ we can estimate the internal cohesion for asteroids. Assuming an average $\rho = 1.93 \text{ g cm}^{-3}$ for V-type asteroids (Carry 2012), a cohesion of 47 ± 20 Pa results for 2005 EC₁₂₇.¹⁷ This modest value is comparable with that of the other large SFRs (see Table 2) and is also nearly in the cohesion range of lunar regolith, i.e., 100–1000 Pa (Mitchell et al. 1974).

As shown by Holsapple (2007), the size-dependent cohesion would allow large SFRs to be present in the transition zone between monolithic and rubble-pile asteroids. However, only six large SFRs have been reported to date (including this work). This number is very small when compared with the number of

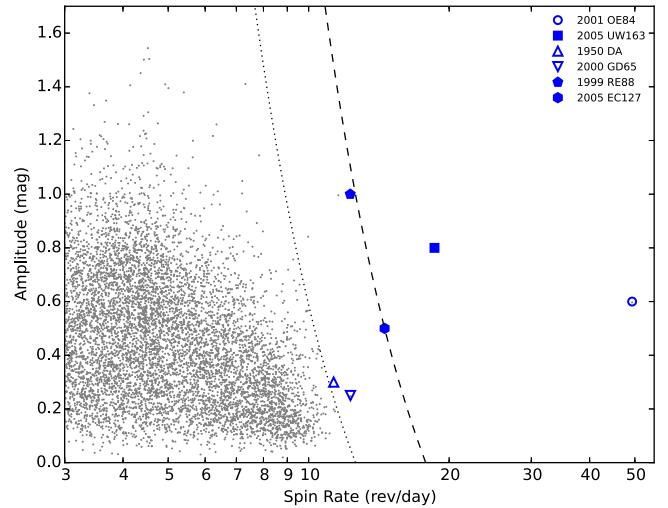


Figure 3. Asteroid light-curve amplitude vs. spin rate. The gray dots are LCDB objects with reliable rotation periods. The blue symbols denote the six reported large SFRs, where the filled symbols were discovered by the iPTF. The dashed and dotted lines represent the estimated spin rate limits for rubble-pile asteroids of bulk densities of $\rho = 6$ and 3 g cm^{-3} , respectively, using $P \sim 3.3\sqrt{(1 + \Delta m)/\rho}$ hr, where Δm is the light-curve amplitude (Harris 1996). Assuming a rubble-pile structure, the estimated bulk density of 2005 EC₁₂₇ (blue hexagon) would be $\sim 6 \text{ g cm}^{-3}$.

large fast rotators (i.e., 738 objects in the LCDB). The reason for the rarity in detecting large SFRs from previous studies (i.e., the sparse number of large SFRs in the transition zone in Figure 4) could be that (a) the rotation periods are difficult to obtain for large SFRs due to their small diameters (i.e., faint brightness) or (b) the population size of large SFRs is intrinsically small. Therefore, a survey of asteroid rotation period with a larger sky coverage and deeper limiting magnitude can help to resolve the aforementioned question. If it is the latter case, these large SFRs might be monoliths, which have relatively large diameters and unusual collision histories.

We also note that none of the six reported large SFRs is classified as C-type asteroids. Therefore, any discovery of a large C-type SFR would fill out this taxonomic vacancy and help to understand the formation of large SFRs. In addition, the determination of the upper limit of the SFR diameter is also important for understanding asteroid interior structure since this can constrain the upper limit of the internal cohesion of asteroids.

5. Summary and Conclusions

(144977) 2005 EC₁₂₇ is consistent with a V-/A-type inner-main-belt asteroid, based on our follow-up spectroscopic observations, with a diameter estimated to be 0.6 ± 0.1 km from the standard brightness/albedo relation. Its rotation period was first determined to be 1.64 ± 0.01 hr from our iPTF asteroid rotation-period survey and then was confirmed as 1.65 ± 0.01 hr by the follow-up observations reported here using the LOT. We categorize 2005 EC₁₂₇ as a large SFR, given its size and since its rotation period is less than the 2.2 hr spin barrier.

Considering its 0.6 km diameter, 2005 EC₁₂₇ is most likely a rubble-pile asteroid. For 2005 EC₁₂₇ to survive under its super-fast rotation, either an internal cohesion of 47 ± 20 Pa or an unusually high bulk density of $\rho \sim 6 \text{ g cm}^{-3}$ is required. However, the latter case is very unlikely for large asteroids, and more so for V-/A-type asteroids, as 2005 EC₁₂₇ has been classified. Only six large SFRs have been reported in the

¹⁵ A G slope of 0.24 for S-type asteroids (Pravec et al. 2012) would make the H magnitude ~ 0.03 mag fainter, which is equivalent to a ~ 0.01 km diameter difference, and within the uncertainty of our estimation.

¹⁶ The detailed calculation is given in Chang et al. (2016). This method has been widely used, e.g., in Holsapple (2007), Rozitis et al. (2014), and Polishook et al. (2016).

¹⁷ For an A-type asteroid with average density $\rho = 3.73 \text{ g cm}^{-3}$ (Carry 2012), the cohesion would be 52 Pa.

Table 2
Confirmed Large SFRs to Date

	Asteroid	Tax.	Per. (hr)	Δm (mag)	Dia. (km)	H (mag)	Coh. (Pa)	a (au)	e	i ($^{\circ}$)	Ω ($^{\circ}$)	ω ($^{\circ}$)	Reference
(144977)	2005 EC ₁₂₇	V/A	1.65 \pm 0.01	0.5	0.6 \pm 0.1	17.8 \pm 0.1	47 \pm 30	2.21	0.17	4.75	336.9	312.8	This work
(455213)	2001 OE ₈₄	S	0.49 \pm 0.00	0.5	0.7 \pm 0.1	18.3 \pm 0.2	\sim 1500 ^a	2.28	0.47	9.34	32.2	2.8	Pravec et al. (2002)
(335433)	2005 UW ₁₆₃	V	1.29 \pm 0.01	0.8	0.6 \pm 0.3	17.7 \pm 0.3	\sim 200 ^a	2.39	0.15	1.62	224.6	183.6	Chang et al. (2014b)
(29075)	1950 DA	M	2.12 \pm 0.00	0.2 ^b	1.3 \pm 0.1	16.8 \pm 0.2	64 \pm 20	1.70	0.51	12.17	356.7	312.8	Rozitis et al. (2014)
(60716)	2000 GD ₆₅	S	1.95 \pm 0.00	0.3	2.0 \pm 0.6	15.6 \pm 0.5	150–450	2.42	0.10	3.17	42.1	162.4	Polishook et al. (2016)
(40511)	1999 RE ₈₈	S	1.96 \pm 0.01	1.0	1.9 \pm 0.3	16.4 \pm 0.3	780 \pm 500	2.38	0.17	2.04	341.6	279.8	Chang et al. (2016)

Notes. The orbital elements were obtained from the MPC website, <http://www.minorplanetcenter.net/iau/mpc.html>.

^a The cohesion is adopted from Chang et al. (2016).

^b Δm is adopted from Busch et al. (2007).

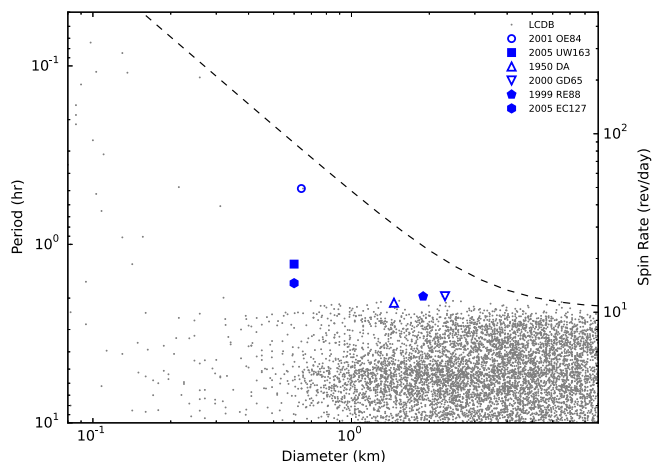


Figure 4. Asteroid rotation period (spin rate) vs. diameter. The symbol assignments are the same as used in Figure 3. The large SFRs have somewhat smaller periods than the spin barrier at 2.2 hr. The dashed line is the predicted spin limit with cohesion $\kappa = k\bar{r}^{-1/2}$, where the strength coefficient $k = 2.25 \times 10^7$ dynes $\text{cm}^{-3/2}$ and \bar{r} is the mean radius (Holsapple 2007).

literature, including 2005 EC₁₂₇, the subject of this work. This number is very small compared with the number of existing large fast rotators. Therefore, future surveys will help to reveal whether this rarity in detection is due to the intrinsically small population size of large SFRs. Moreover, none of the known SFRs have been classified as C-type asteroids, and the discovery of a large SFR of this type in future work would be an interesting development to further our understanding of the formation of large super-fast rotators.

This work is supported in part by the Ministry of Science and Technology of Taiwan under grants MOST 104-2112-M-008-014-MY3, MOST 104-2119-M-008-024, and MOST 105-2112-M-008-002-MY3, and also by Macau Science and Technology Fund No. 017/2014/A1 of MSAR. We are thankful for the indispensable support provided by the staff of the Lulin Observatory and the staff of the Palomar Observatory. We thank the anonymous referee for useful suggestions and comments.

References

Bellm, E. C., & Sesar, B. 2016, pyraf-dbsp: Reduction pipeline for the Palomar Double Beam Spectrograph, Astrophysics Source Code Library, ascl:1602.002
 Bertin, E., & Arnouts, S. 1996, *A&AS*, 117, 393

Bowell, E., Hapke, B., Domingue, D., et al. 1989, in Asteroids II (Tucson, AZ: Univ. Arizona Press), 524
 Busch, M. W., Giorgini, J. D., Ostro, S. J., et al. 2007, *Icar*, 190, 608
 Carry, B. 2012, *P&SS*, 73, 98
 Chang, C.-K., Ip, W.-H., Lin, H.-W., et al. 2014a, *ApJ*, 788, 17
 Chang, C.-K., Ip, W.-H., Lin, H.-W., et al. 2015, *ApJS*, 219, 27
 Chang, C.-K., Lin, H.-W., Ip, W.-H., et al. 2016, *ApJS*, 227, 20
 Chang, C.-K., Waszczak, A., Lin, H.-W., et al. 2014b, *ApJL*, 791, LL35
 Cleveland, W. S. 1979, *J. Am. Stat. Assoc.*, 74, 829
 DeMeo, F. E., Binzel, R. P., Slivan, S. M., & Bus, S. J. 2009, *Icar*, 202, 160
 DeMeo, F. E., & Carry, B. 2013, *Icar*, 226, 723
 Dermawan, B., Nakamura, T., & Yoshida, F. 2011, *PASJ*, 63, 555
 Grillmair, C. J., Laher, R., Surace, J., et al. 2010, in ASP Conf. Ser. 434, Astronomical Data Analysis Software and Systems XIX, ed. Y. Mizumoto, K.-I. Morita, & M. Ohishi (San Francisco, CA: ASP), 28
 Harris, A. W., & Lagerros, J. S. V. 2002, in Asteroids III, ed. W. F. Bottke Jr., et al. (Tucson, AZ: Univ. Arizona Press), 205
 Harris, A. W., Pravec, P., Galád, A., et al. 2014, *Icar*, 235, 55
 Harris, A. W., Young, J. W., Bowell, E., et al. 1989, *Icar*, 77, 171
 Harris, A. W. 1996, *LPSC*, 27, 493
 Holsapple, K. A. 2007, *Icar*, 187, 500
 Kinoshita, D., Chen, C.-W., Lin, H.-C., et al. 2005, *ChJAA*, 5, 315
 Kurucz, R. L., Furenlid, I., Brault, J., & Testerman, L. 1984, National Solar Observatory Atlas (Sunspot, NM: National Solar Observatory)
 Laher, R. R., Surace, J., Grillmair, C. J., et al. 2014, *PASP*, 126, 674
 Law, N. M., Dekany, R. G., Rahmer, G., et al. 2010, *Proc. SPIE*, 7735, 77353M
 Law, N. M., Kulkarni, S. R., Dekany, R. G., et al. 2009, *PASP*, 121, 1395
 Lin, H. W., Yoshida, F., Chen, Y. T., Ip, W. H., & Chang, C. K. 2015, *Icar*, 254, 202
 Magnier, E. A., Schlafly, E. F., Finkbeiner, D. P., et al. 2016, arXiv:1612.05242
 Masiero, J., Jedicke, R., Āurech, J., et al. 2009, *Icar*, 204, 145
 Masiero, J. R., Mainzer, A. K., Grav, T., et al. 2011, *ApJ*, 741, 68
 Mitchell, J. K., Houston, W. N., Carrier, W. D., & Costes, N. C. 1974, Apollo Soil Mechanics Experiment S-200 Final Report 7285 (Berkeley, CA: Univ. California)
 Ofek, E. O., Laher, R., Law, N., et al. 2012a, *PASP*, 124, 62
 Ofek, E. O., Laher, R., Surace, J., et al. 2012b, *PASP*, 124, 854
 Oke, J. B., & Gunn, J. E. 1982, *PASP*, 94, 586
 Polishook, D., Moskovitz, N., Binzel, R. P., et al. 2016, *Icar*, 267, 243
 Polishook, D., Ofek, E. O., Waszczak, A., et al. 2012, *MNRAS*, 421, 2094
 Pravec, P., Harris, A. W., Kušnirák, P., Galád, A., & Hornoch, K. 2012, *Icar*, 221, 365
 Pravec, P., Kušnirák, P., Šarounová, L., et al. 2002, in Asteroids, Comets, and Meteors: ACM 2002, ed. B. Warmbein (ESA SP-500; Noordwijk: ESA), 743
 Rau, A., Kulkarni, S. R., Law, N. M., et al. 2009, *PASP*, 121, 1334
 Rozitis, B., MacLennan, E., & Emery, J. P. 2014, *Nature*, 512, 174
 Sánchez, P., & Scheeres, D. J. 2014, *M&PS*, 49, 788
 Vereš, P., Jedicke, R., Denneau, L., et al. 2012, *PASP*, 124, 1197
 Warner, B. D., Harris, A. W., & Pravec, P. 2009, *Icar*, 202, 134
 York, D. G., Adelman, J., Anderson, J. E., Jr., et al. 2000, *AJ*, 120, 1579